Letter

Efficient tomography of coherent optical detectors

Xinyu Chen, Feixiang Xu, Huichao Xu, and Lijian Zhang*

National Laboratory of Solid State Microstructures and College of Engineering and Applied Sciences, Nanjing University, Nanjing 210093, China

and Collaborative Innovation Center of Advanced Microstructures Nanjing University, Nanjing 210093, China

(Received 14 August 2022; accepted 16 November 2022; published 30 November 2022)

We propose an efficient tomography method to address the reconstruction complexity of any general quantum coherent-optical detectors. By extracting the linear loss from the entire detection system, we obtain the effective positive-operator-valued measure in matrix representations with a much smaller size. We apply this method to reconstruct a typical coherent detector: the weak-field homodyne detector. The method also highlights the effects of linear loss on nonclassical features of coherent optical detectors.

DOI: 10.1103/PhysRevA.106.L051702

I. INTRODUCTION

Quantum detector plays a fundamental role in investigating and controlling various quantum systems [1]. The complete knowledge of the detector relies on the characterization of its positive-operator-valued measure (POVM) that links the input states to the classical output. A typical technique of characterizing any quantum detector is called quantum detector tomography (QDT) [2–5], which reconstructs the POVM from the measured outcome statistics by using a set of tomographically complete states as the probe. QDT has been applied to avalanche photodiodes (APDs) [6], time-multiplexed detectors (TMDs) [3,7,8], and superconducting nanowire detectors [9–11]. These detectors are phase insensitive, i.e., they cannot respond to the coherence among photon-number states. Since the matrix representations of the POVM are diagonal in the photon-number basis, they are relatively straightforward to reconstruct.

However, for coherent optical detectors such as weak-field homodyne detectors [12,13], which have unique characteristics in bridging particle and wave sensitivity, the POVM elements will have nonzero off-diagonal entries in their matrix representations. These detectors are phase sensitive and can access quantum coherence among photon-number states [14,15], which are of vital importance in applications such as quantum state engineering [16,17], coherent optical communication [18,19], continuous variable quantum key distribution [20,21], and fundamental investigations on quantum mechanics [22]. The reconstruction of these POVMs is more difficult than that of incoherent detectors since the number of parameters to be estimated is proportional to d^2, where d is the dimension of the Hilbert space determined by the number of photons that saturate the detector. For practical detectors with a large dynamic range, d can range from 10^2 to 10^5, and then d^2 from 10^4 to 10^{10}. Thus, the QDT of coherent optical detectors is much more challenging.

To characterize the coherent optical detectors, a recursive reconstruction method [23] of QDT was proposed, which reduced the computational complexity from quadratic to linear per recursion with respect to dimension d. Lately, an improved reconstruction method was introduced in studying the coherence of a weak-field homodyne APD [24]. The method adopted the approach which dealt with the diagonal and off-diagonal entries of the POVM elements but reconstructed them in a run. The omission of the recursive process in the improved method brought about higher reconstruction efficiency and accuracy. However, both the methods do not decrease the total size of the POVM, thus the total computation burden is still large. To avoid numerical instability in the reconstruction of realistic detectors, suitable regularization conditions are introduced to obtain a smooth POVM in these methods. For coherent detectors with complex structures, the characterization calls for a more efficient tomography method.

For the coherent optical detectors, linear loss is one of the major effects accounting for the large number of free parameters in the POVM elements and then huge computation work in the QDT of them. It was shown that the linear loss can be decoupled from the nonlinear response in the characterization of incoherent detectors [9]. However, whether this idea can be applied to the characterization of coherent detectors remains elusive due to the sophisticated effect of linear loss on the response of coherent detectors. In this work, we propose an efficient method to decouple the linear loss from the response of coherent detectors and reduce the reconstruction complexity greatly, which is model independent and generally applicable to all coherent detectors. By extracting the linear loss, we obtain the effective POVM with a significantly smaller size. We employ this method to characterize a typical coherent detector: the weak-field homodyne detector. When taking into account the linear loss, the results show an average fidelity of over 99% with the POVMs reconstructed by the conventional reconstruction method [24]. Moreover, our method highlights the effects of linear loss on nonclassical features of coherent optical detectors.

II. DESCRIPTION OF THE ALGORITHM

In the QDT theory, with a set of known probe states $\{\hat{\rho}_m\}$ ($m = 1, 2, \ldots, M$, where M is the total number of probe

*Corresponding author: lijian.zhang@nju.edu.cn

states) incident on a quantum detector, we collect the measurement outcomes of the detector [3]. The link is given by the Born rule, which indicates that the probability for an outcome n is

$$p_{n|m} = \mathrm{tr}(\hat{\rho}_m \hat{\Pi}_n), \tag{1}$$

where $\{\hat{\Pi}_n\}$ is the POVM of the detector with $n = 0, 1, \ldots, N-1$, and N is the number of outcomes for the detector. To determine $\{\hat{\Pi}_n\}$ from Eq. (1), the set of probe states should be tomographically complete. In practice, one candidate is the set of coherent states $|\alpha_m\rangle$, which can be generated by modulating the output of a laser. We expand $\{\hat{\Pi}_n\}$ and $|\alpha_m\rangle$ in the Fock basis and truncate the expansion at the number of photons $d-1$ that saturate the detector

$$\hat{\Pi}_n = \sum_{j,k=0}^{d-1} \pi_n^{j,k} |j\rangle\langle k|, \tag{2}$$

and

$$|\alpha_m\rangle = e^{-|\alpha_m|^2/2} \sum_{j=0}^{d-1} \frac{|\alpha_m|^j}{\sqrt{j!}} e^{ij\theta_m} |j\rangle. \tag{3}$$

Then we can rewrite Eq. (1) as

$$p_{n|m} = e^{-|\alpha_m|^2} \sum_{j,k=0}^{d-1} \frac{|\alpha_m|^{j+k}}{\sqrt{j!k!}} e^{i(k-j)\theta_m} \pi_n^{j,k}. \tag{4}$$

We relabel the basis elements using an index parameter t ($1 \leqslant t \leqslant d^2$), and define $j(t) = (t-1) \bmod d$ and $k(t) = [t - j(t) - 1] \bmod d$. Equation (4) can be rearranged in a matrix form

$$P = \tilde{F}\tilde{\Pi}, \tag{5}$$

where P is an $M \times N$ matrix containing the measured probabilities with elements $P^{m,n} = p_{n|m}$, $\tilde{F}$ is an $M \times d^2$ matrix that contains the probe states information with elements

$$\tilde{F}^{m,t} = e^{-|\alpha_m|^2} \frac{|\alpha_m|^{j(t)+k(t)}}{\sqrt{j(t)!k(t)!}} e^{i[k(t)-j(t)]\theta_m}, \tag{6}$$

and $\tilde{\Pi}$ is a $d^2 \times N$ matrix that contains the unknown POVM with elements $\tilde{\Pi}^{t,n} = \pi_n^{j(t),k(t)}$. Due to the experimental imperfections, instead of directly solving Eq. (5), we can solve a convex quadratic optimization problem

$$\begin{aligned} &\text{minimize:} \quad \|P - \tilde{F}\tilde{\Pi}\|_2 + g(\tilde{\Pi}), \\ &\text{subject to:} \quad \hat{\Pi}_n \geqslant 0, \ \sum_{n=0}^{N-1} \hat{\Pi}_n = \hat{I}, \end{aligned} \tag{7}$$

where $\|A\|_2 = \sqrt{\mathrm{tr}(A^\dagger A)}$ is the Frobenius norm, $g(\tilde{\Pi})$ is a regularization function [3], and $\hat{I}$ is the identity operator. Equation (7) is a semi-definite problem and the solution can be obtained numerically.

Due to the large size of P, $\tilde{F}$, and $\tilde{\Pi}$, to reduce the reconstruction complexity, an improved reconstruction algorithm [24] was developed by reconstructing the POVM up to l leading diagonals ($0 \leqslant l \leqslant d-1$). This is realized by transforming each POVM element into a column vector with all leading diagonals in arrangement successively. The nth column of $\tilde{\Pi}$ contains the relevant part of $\hat{\Pi}_n$, i.e., the diagonal entries of $\hat{\Pi}_n$, followed by the first off-diagonal above, the first off-diagonal below, the second off-diagonal above, and so on, and the lth off-diagonal below. The remaining off-diagonal entries are assumed to be zero, which is a good approximation providing enough of diagonals were taken into account. The rearranged matrix $\tilde{\Pi}$ has a size of $[d + (2d - l - 1)l] \times N$ and can be reconstructed in a run by using the convex optimization approach in Eq. (7). This algorithm does not reduce the dimension of the POVM, so it still holds a large computation burden for coherent detectors with complex structures.

Here, we propose a more efficient method to reconstruct the coherent optical detectors. Our aim is to separate the linear loss from the original POVM element of the detector. The linear loss leads to more unknown parameters in coherent detectors than in incoherent detectors. Since the dimension of the POVM is inversely proportional to the efficiency of the detector, if we can extract an efficiency parameter η from the POVM, we can reduce the size of matrix $\hat{\Pi}$ and the number of the parameters to be estimated by a factor of about η^2. Since the main diagonal of the matrix representation of the POVM given in Eq. (2) involves the response to the photon number statistics and the linear loss can be viewed as a reduction of the input photon numbers, we can extract the efficiency parameter η that accounts for the linear loss from the main diagonal and obtain the effective POVM element with a smaller size.

In practice, the probe states are prepared with M_a different amplitudes and M_p different phases for each amplitude. Then we have $M = M_a M_p$ of the states with the complex amplitudes $\alpha_{u,v} = |\alpha_u| e^{i\theta_v}$, with $u = 1, \ldots, M_a$ and $v = 1, \ldots, M_p$. We first integrate over the probe state phase θ. Since

$$\int_0^{2\pi} e^{i(k-j)\theta} d\theta = 2\pi \delta_{k,j}, \tag{8}$$

using Eq. (4), we obtain

$$\frac{1}{2\pi} \int_0^{2\pi} p_{n|m} d\theta = e^{-\eta|\alpha_u|^2} \sum_{s=0} \frac{(\eta|\alpha_u|^2)^s}{s!} q_s. \tag{9}$$

Here η is the extracted efficiency parameter and $\{q_s\}$ are positive real parameters, which are all between 0 and 1. The left side of Eq. (9) is a partial integration of the measured probabilities that can be obtained by numerical approximation, while the right side involves the main diagonal of the POVM. We decompose the main diagonal entries into an efficiency parameter η conducted on input photon numbers and some remainders $\{q_s\}$ representing the nonlinear parts. Then we change the left integration to a summation with

$$\frac{1}{2\pi} \int_0^{2\pi} p_{n|m} d\theta \approx \frac{1}{m_p} \sum_{v=1}^{m_p} p_{n|\alpha_{u,v}}. \tag{10}$$

Using Eqs. (9) and (10), we can fit the unknown parameters η and $\{q_s\}$ to the measured probabilities as a function of $|\alpha_u|^2$ (the photon number of probe states). The computational complexity is $O(d)$. To avoid overparametrizing the system, we choose the minimum number of $\{q_s\}$ to best fit our data in

Eq. (9). With the estimated efficiency $\eta_{\rm est}$, we insert it into

$$p_{n|\alpha_{u,v}} = e^{-\eta_{\rm est}|\alpha_u|^2} \sum_{j,k=0}^{d'-1} \frac{(\sqrt{\eta_{\rm est}}|\alpha_u|)^{j+k}}{\sqrt{j!k!}} e^{i(k-j)\theta_v} \pi_n^{{\rm eff}(j,k)}. \quad (11)$$

Here, we have

$$\hat{\Pi}_n^{\rm eff} = \sum_{j,k=0}^{d'-1} \pi_n^{{\rm eff}(j,k)} |j\rangle\langle k|, \quad (12)$$

where d' is the new dimension of the Hilbert space to describe the effective POVM.

Instead of taking the direct inversion of Eq. (11), which may give unphysical POVM elements, we adopt the convex optimization method

$$\begin{aligned} &\text{minimize:} \quad \|P - \tilde{F}^{\rm eff}\tilde{\Pi}^{\rm eff}\|_2, \\ &\text{subject to:} \quad \hat{\Pi}_n^{\rm eff} \geqslant 0, \ \sum_{n=0}^{N-1} \hat{\Pi}_n^{\rm eff} = \hat{I}. \end{aligned} \quad (13)$$

Here the matrix form of $\tilde{\Pi}^{\rm eff}$ is constructed in the same way as the improved reconstruction method. By rearranging the leading diagonal entries of the effective POVM elements in a series connection, we use a index number r to define the corresponding matrix form. According to $\tilde{\Pi}^{{\rm eff}(r,n)} = \pi_n^{[(j(r),k(r)]}$ and

$$\tilde{F}^{{\rm eff}(m,r)} = e^{-\eta_{\rm est}|\alpha_u|^2} \frac{\sqrt{\eta_{\rm est}}|\alpha_u|^{j(r)+k(r)}}{\sqrt{j(r)!k(r)!}} e^{i[k(r)-j(r)]\theta_v}, \quad (14)$$

we can reconstruct the effective POVM elements efficiently using Eq. (13). Since the linear loss was separated out from the original POVM elements, the smoothness requirement of the effective POVM can be removed. This also makes the optimization procedure much simpler.

III. RECONSTRUCTION OF THE WEAK-FIELD HOMODYNE DETECTORS

We apply the method to reconstruct a typical kind of coherent detectors: the weak-field homodyne detector. The configuration of such a detector and its schematic tomography setup is shown in Fig. 1. A set of probe states is generated from the output of a laser followed by the phase modulation and amplitude modulation, then it is injected into a weak-field homodyne detector, which is represented by the dotted box. The detector combines the probe states with a local oscillator (LO), usually a weak coherent state $|\alpha_{\rm LO}\rangle$ at a beam splitter with transmissivity T, followed by an APD or a photon-number-resolving detector (PNRD). The POVM of a weak-field homodyne detector is determined by the beam-splitting ratio, the amplitude and phase of the LO, and the detailed response of APD or PNRD. In addition, the mode overlap between probe states and LO and different transmission loss on them may also affect the POVM.

Here, we apply our method to characterize both the weak-field homodyne APD and PNRD. The experimental data are taken from Ref. [13]. We first present the reconstruction results of a weak-field homodyne APD (with a detection efficiency of 39% for APD). The APD only registers click and no-click event. For $|\alpha_{\rm LO}|^2 = 0.8$ photons, the LO phase of zero, a beam splitter transmissivity of 65.5%, and a mode overlap of 0.99, we reconstruct the effective POVM element for the no-click event of the weak-field homodyne APD, which is depicted in Fig. 2. In the estimation of $\eta_{\rm est}$, we need to use a sufficient number of probe phases for an accurate reconstruction, as was given in Ref. [23]. The number of the experimental data is $M_a = 110$ and $M_p = 40$. We obtain $\eta_{\rm est} = 0.2761$ and the relative error of the reconstruction with $\|P_0 - \tilde{F}^{\rm eff}\tilde{\Pi}_0^{\rm eff}\|_2/\|P_0\|_2 = 0.6\%$. The dimension of the effective POVM element is truncated at $d' = 4$. As a comparison, with the previous algorithm [23,24], the dimension of the reconstructed POVM element is above 30. The method has greatly reduced the computation complexity. In addition, to

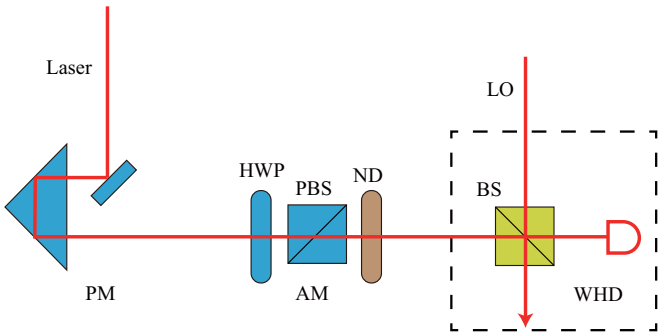

FIG. 1. The configuration of a weak-field homodyne detector and its schematic tomography setup. The probe states are generated with the laser output passing through phase-modulation (PM) and amplitude-modulation (AM) devices and are injected into the weak-field homodyne detector (WHD). The phases of the probe states can be set by a piezotranslator. The magnitudes of the probe states can be controlled by a half-wave plate (HWP) followed by a polarizing beam splitter (PBS) and neutral density (ND) filters. The schematic of WHD is shown in the dotted box. The WHD combines the probe states with a local oscillator (LO) at a beam splitter (BS), followed by an intensity detector such as an APD or PNRD.

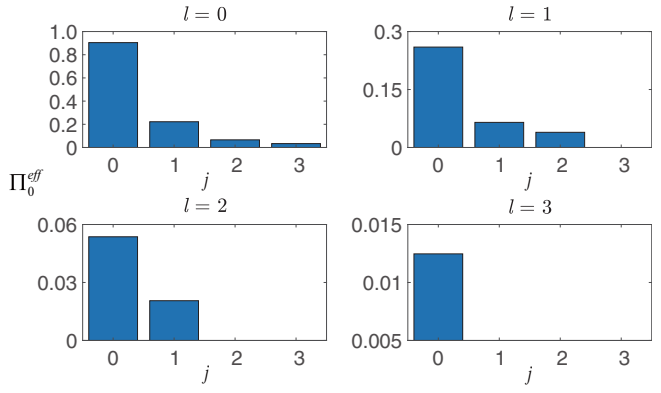

FIG. 2. Reconstructed effective POVM element for the no-click event $\hat{\Pi}_0^{\rm eff}$ of a weak-field homodyne APD with $|\alpha_{\rm LO}|^2 = 0.8$ photons, LO phase of zero, transmissivity of 65.5% for the beam splitter, detection efficiency of 39% for the APD and a mode overlap of 0.99 between the input states and LO. We truncate the dimension at $d' = 4$ and show the lth leading diagonals $\pi_0^{{\rm eff}(j,j+l)} = \langle j|\hat{\Pi}_0^{\rm eff}|j+l\rangle$ of the POVM element from $l = 0$ to $l = 3$. Here we have $\eta_{est} = 0.2761$ and a relative error for the reconstruction of 0.6%.

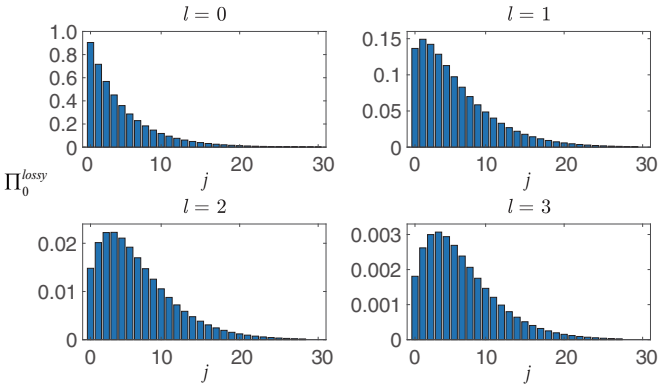

FIG. 3. The overall lossy POVM element $\hat{\Pi}_0^{\text{lossy}}$ by incorporating the estimated loss into the effective POVM element for the no-click event of a weak-field homodyne APD. We truncate the photon number at 30 and show the lth leading diagonals $\pi_0^{\text{lossy}(j,j+l)} = \langle j|\hat{\Pi}_0^{\text{lossy}}|j+l\rangle$ of the POVM element from $l=0$ to $l=3$. The result has a fidelity of 99.67% with the one reconstructed with a conventional reconstruction algorithm.

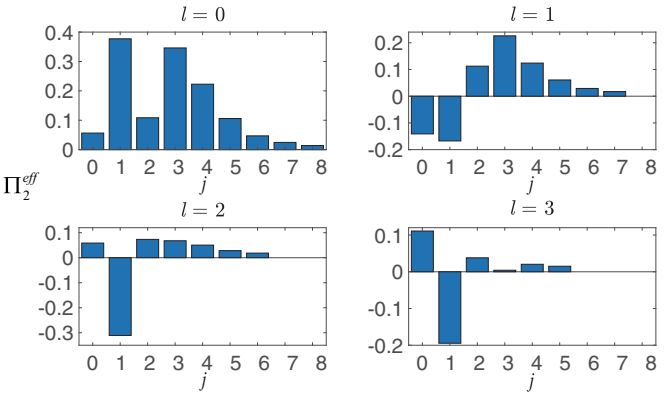

FIG. 4. Reconstructed effective POVM element for the two-click event $\hat{\Pi}_2^{\text{eff}}$ of a weak-field homodyne PNRD (with $|\alpha_{\text{LO}}|^2 = 5$ photons, LO phase of zero, a beam splitter transmissivity of 65.5%, mode overlap of 99%, and a detection efficiency of 24% for a time-multiplexed detector with $N=9$ outputs). We truncate the dimension at $d'=9$ and show the lth leading diagonals $\pi_2^{\text{eff}(j,j+l)} = \langle j|\hat{\Pi}_2^{\text{eff}}|j+l\rangle$ of the POVM element from $l=0$ to $l=3$. Here we have $\eta_{\text{est}} = 0.1382$ and a relative error for the reconstruction of 1.3%.

demonstrate the validity, we incorporate η_{est} into $\hat{\Pi}_0^{\text{eff}}$ and obtain the overall lossy POVM element $\hat{\Pi}_0^{\text{lossy}}$, which is shown in Fig. 3. We calculate the fidelity between the overall lossy POVM element and the one reconstructed using the conventional reconstruction algorithm $\hat{\Pi}_0$ [24]

$$F = \left[\text{tr}\left(\sqrt{\hat{\Pi}_0}\hat{\Pi}_0^{\text{lossy}}\sqrt{\hat{\Pi}_0}\right)^{1/2}\right]^2 / \text{tr}(\hat{\Pi}_0)\text{tr}\left(\hat{\Pi}_0^{\text{lossy}}\right), \qquad (15)$$

which is 99.67%. This fidelity confirms the accuracy of our reconstruction algorithm.

We also apply our method to reconstruct the POVM of a weak-field homodyne PNRD, which is of vital value due to its combination of photon number resolution and phase sensitivity [12,25]. The weak-field homodyne PNRD has $|\alpha_{\text{LO}}|^2$ of five photons, LO phase of zero, a beam splitter transmissivity of 65.5%, the mode overlap of 99% between the input states and LO, and a detection efficiency of 24% for a time-multiplexed detector with $N=9$ outcomes [26,27]. Here we have $M_a = 865$ and $M_p = 40$. To fully characterize such a weak-field homodyne PNRD, the conventional recursive algorithm [13] involves a dimension of $d = 450$. However, with our method, the effective POVM element has a dimension d' of no more than 15. We reconstructed the effective POVM element for the two-click event $\hat{\Pi}_2^{\text{eff}}$, which is shown in Fig. 4. We obtain $\eta_{\text{est}} = 0.1382$ and the relative error of the reconstruction is 1.3%. The overall lossy POVM element $\hat{\Pi}_2^{\text{lossy}}$ is depicted in Fig. 5, which has a fidelity of 99.81% with the reconstructed POVM element using the conventional reconstruction algorithm [24]. The result again confirms the accuracy of our method.

IV. EFFECTS OF LINEAR LOSS IN NONCLASSICAL FEATURES OF COHERENT DETECTORS

By decoupling the loss from the POVM, our method not only reduces the complexity of the reconstruction, but also allows to investigate the effect of loss on nonclassical features of the POVM. The ability to detect coherence from the measurement statistics is one of the most significant features of optical coherent detectors [24]. A method to evaluate the coherence of a measurement was presented in Refs. [24,28]. It was conducted by mapping the measurement to a trace-preserving operation and calculating the coherence of operation using two functionals (i.e., the diamond measure and the nonstochasticity in detection measure). After we separate the linear loss from the original POVM elements of the weak-field homodyne APD, we obtain a coherence value increased from 0.5058 to 0.5402 using the two measures above (two measures yields the same result for a weak-field homodyne APD). It is known that the off-diagonal entries determine the coherence of the POVMs. We infer from Fig. 2 that, when we extract the linear loss, the increased off-diagonal values indicate an increase of the coherence value of the detector.

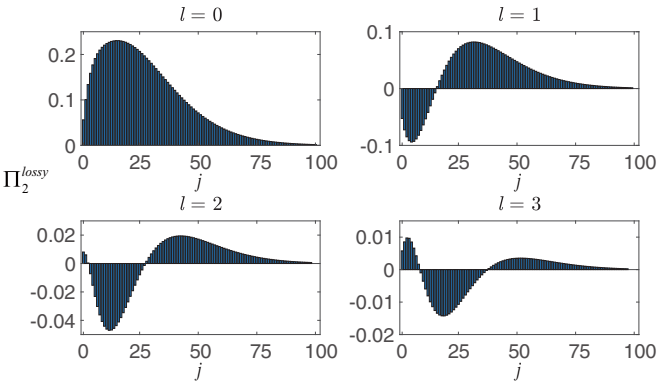

FIG. 5. The overall lossy POVM element $\hat{\Pi}_2^{\text{lossy}}$ by incorporating the estimated loss into the effective POVM element for the two-click event of a weak-field homodyne PNRD. We truncate the photon number at 100 and show the lth leading diagonals $\pi_2^{\text{lossy}(j,j+l)} = \langle j|\hat{\Pi}_2^{\text{lossy}}|j+l\rangle$ of the POVM element from $l=0$ to $l=3$. The result has a fidelity of 99.81% with the one reconstructed with a conventional reconstruction algorithm.

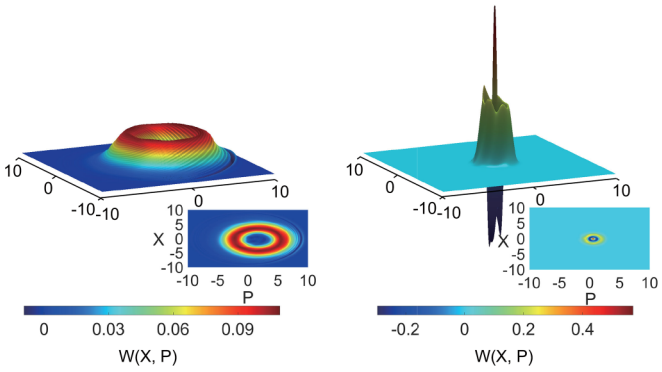

FIG. 6. Wigner function and the corresponding contour plot (inset) for (left) the original POVM element and (right) the effective POVM element of the two-click weak-field homodyne PNRD. The non-Gaussian characteristic is evident from the negative regions. The higher negativity in the right Wigner function indicates the higher non-Gaussianity of the effective POVM element.

The result confirms that linear loss leads to decoherence of the optical coherent detectors. Measurement with non-Gaussian representation in phase space plays a vital role in quantum information processing [29,30]. The non-Gaussian feature of the detection can be explored with the Wigner function of its POVM. Here, We show the Wigner functions of the reconstructed original and effective two-click POVM elements, respectively, for the weak-field homodyne PNRD in Fig. 6. The original POVM shows a broadened and flattened Wigner function since the linear loss in the detector leads to the lower sensitivity to small photon numbers. The Wigner function of the effective POVM is closer to that of a displaced two-photon Fock state with a displacement of 0.6. The overlap between the Wigner function of the effective POVM element (right) and that of a displaced two-photon Fock-state is 0.9966 [31]. Similar to the Wigner function of a quantum state [32], we calculate the negative volume of the Wigner function of a measurement operator, which is defined by $\delta = \int\int |W(X,P)|dXdP - \int\int W(X,P)dXdP$. δ is an indicator of the non-Gaussianity. The results for the original and effective POVM elements are 0.0109 and 0.6748, respectively. This indicates linear loss greatly decreases the non-Gaussianity of the detector. This finding has particular influence on not only the detection, but also the preparation [16] of nonclassical states with coherent optical detectors.

V. CONCLUSION

Optical coherent detectors are essential to both quantum and classical optical applications [17,19,22,33]. The explorations of these applications rely on accurate knowledge of the detectors. For coherent detectors with complex structures and high photon-number-resolving capability, the number of unknown parameters grows significantly, which makes the tomography much more challenging. In this work, we propose and demonstrate a method to reconstruct the coherent optical detectors, which exhibits high accuracy and is applicable to the experimental system with practical statistical fluctuations. We manage to separate the linear loss from the original POVM and obtain the effective POVM in a much smaller size, which, together with the linear loss, fully characterizes the coherent optical detector. For a practical detector, our method can reduce the reconstruction complexity by two orders of magnitude. In addition, the method reveals the effects of linear loss on studying the nonclassicality of coherent detectors. Our work provides an efficient solution to the benchmarking of the performance of coherent optical detectors for widespread use in quantum information applications [34,35]. We also expect this method will facilitate the design of coherent detectors with more complex structures.

ACKNOWLEDGMENTS

This work was supported by the National Key Research and Development Program of China (Grants No. 2019YFA0308704 and No. 2018YFA0306202), National Natural Science Foundation of China (Grants No. 61975077, No. 91836303, and No. 11690032), and Fundamental Research Funds for the Central Universities (Grant No. 020414380175). We also thank J. J. Renema for helpful discussions.

[1] V. B. Braginsky and F. Y. Khalili, *Quantum Measurement* (Cambridge University Press, Cambridge, England, 1995).
[2] A. Luis and L. L. Sánchez-Soto, Phys. Rev. Lett. **83**, 3573 (1999).
[3] J. Lundeen, A. Feito, H. Coldenstrodt-Ronge, K. Pregnell, C. Silberhorn, T. Ralph, J. Eisert, M. Plenio, and I. Walmsley, Nat. Phys. **5**, 27 (2009).
[4] J. Fiurášek, Phys. Rev. A **64**, 024102 (2001).
[5] G. M. D'Ariano, L. Maccone, and P. Lo Presti, Phys. Rev. Lett. **93**, 250407 (2004).
[6] V. D'Auria, N. Lee, T. Amri, C. Fabre, and J. Laurat, Phys. Rev. Lett. **107**, 050504 (2011).
[7] A. Feito, J. Lundeen, H. Coldenstrodt-Ronge, J. Eisert, M. B. Plenio, and I. A. Walmsley, New J. Phys. **11**, 093038 (2009).
[8] H. B. Coldenstrodt-Ronge, J. S. Lundeen, K. L. Pregnell, A. Feito, B. J. Smith, W. Mauerer, C. Silberhorn, J. Eisert, M. B. Plenio, and I. A. Walmsley, J. Mod. Opt. **56**, 432 (2009).
[9] J. Renema, G. Frucci, Z. Zhou, F. Mattioli, A. Gaggero, R. Leoni, M. De Dood, A. Fiore, and M. van Exter, Opt. Express **20**, 2806 (2012).
[10] M. K. Akhlaghi, A. H. Majedi, and J. S. Lundeen, Opt. Express **19**, 21305 (2011).
[11] T. Schapeler, J. P. Höpker, and T. J. Bartley, Opt. Express **28**, 33035 (2020).
[12] G. Puentes, J. S. Lundeen, M. P. A. Branderhorst, H. B. Coldenstrodt-Ronge, B. J. Smith, and I. A. Walmsley, Phys. Rev. Lett. **102**, 080404 (2009).
[13] L. Zhang, H. B. Coldenstrodt-Ronge, A. Datta, G. Puentes, J. S. Lundeen, X.-M. Jin, B. J. Smith, M. B. Plenio, and I. A. Walmsley, Nat. Photonics **6**, 364 (2012).

[14] G. Donati, T. J. Bartley, X.-M. Jin, M.-D. Vidrighin, A. Datta, M. Barbieri, and I. A. Walmsley, Nat. Commun. **5**, 5584 (2014).
[15] V. Cimini, I. Gianani, M. Sbroscia, J. Sperling, and M. Barbieri, Phys. Rev. Res. **1**, 033020 (2019).
[16] G. S. Thekkadath, B. A. Bell, I. A. Walmsley, and A. I. Lvovsky, Quantum **4**, 239 (2020).
[17] E. Bimbard, N. Jain, A. MacRae, and A. Lvovsky, Nat. Photonics **4**, 243 (2010).
[18] K. Tsujino, D. Fukuda, G. Fujii, S. Inoue, M. Fujiwara, M. Takeoka, and M. Sasaki, Phys. Rev. Lett. **106**, 250503 (2011).
[19] F. Becerra, J. Fan, G. Baumgartner, J. Goldhar, J. Kosloski, and A. Migdall, Nat. Photonics **7**, 147 (2013).
[20] Y. Zhang, Z. Chen, S. Pirandola, X. Wang, C. Zhou, B. Chu, Y. Zhao, B. Xu, S. Yu, and H. Guo, Phys. Rev. Lett. **125**, 010502 (2020).
[21] G. Zhang, J. Y. Haw, H. Cai, F. Xu, S. M. Assad, J. F. Fitzsimons, X. Zhou, Y. Zhang, S. Yu, J. Wu, W. Ser, L. C. Kwek, and A. Q. Liu, Nat. Photonics **13**, 839 (2019).
[22] T. Das, M. Karczewski, A. Mandarino, M. Markiewicz, B. Woloncewicz, and M. Żukowski, New J. Phys. **24**, 033017 (2022).
[23] L. Zhang, A. Datta, H. B. Coldenstrodt-Ronge, X.-M. Jin, J. Eisert, M. B. Plenio, and I. A. Walmsley, New J. Phys. **14**, 115005 (2012).
[24] H. Xu, F. Xu, T. Theurer, D. Egloff, Z.-W. Liu, N. Yu, M. B. Plenio, and L. Zhang, Phys. Rev. Lett. **125**, 060404 (2020).
[25] G. S. Thekkadath, D. S. Phillips, J. F. F. Bulmer, W. R. Clements, A. Eckstein, B. A. Bell, J. Lugani, T. A. W. Wolterink, A. Lita, S. W. Nam, T. Gerrits, C. G. Wade, and I. A. Walmsley, Phys. Rev. A **101**, 031801(R) (2020).
[26] D. Achilles, C. Silberhorn, C. Śliwa, K. Banaszek, and I. A. Walmsley, Opt. Lett. **28**, 2387 (2003).
[27] D. Achilles, C. Silberhorn, and I. A. Walmsley, Phys. Rev. Lett. **97**, 043602 (2006).
[28] T. Theurer, D. Egloff, L. Zhang, and M. B. Plenio, Phys. Rev. Lett. **122**, 190405 (2019).
[29] N. C. Menicucci, P. van Loock, M. Gu, C. Weedbrook, T. C. Ralph, and M. A. Nielsen, Phys. Rev. Lett. **97**, 110501 (2006).
[30] S.-W. Ji, J. Lee, J. Park, and H. Nha, Sci. Rep. **6**, 29729 (2016).
[31] U. Leonhardt and H. Paul, Prog. Quantum Electron. **19**, 89 (1995).
[32] A. Kenfack and K. Zyczkowski, J. Opt. B **6**, 396 (2004).
[33] M. Barbieri, PRX Quantum **3**, 010202 (2022).
[34] U. L. Andersen, J. S. Neergaard-Nielsen, P. Van Loock, and A. Furusawa, Nat. Phys. **11**, 713 (2015).
[35] S. L. Braunstein and P. van Loock, Rev. Mod. Phys. **77**, 513 (2005).